ELSEVIER

Journal of Alloys and Compounds 293–295 (1999) 468–471

Journal of ALLOYS AND COMPOUNDS

In situ monitoring of hydrogen absorption–desorption in Pd and $Pd_{77}Ag_{23}$ films by an electrochemical quartz crystal microbalance

S.-Y. Liu[a,*], Y.-H. Kao[b], Y. Oliver Su[b], T.-P. Perng[a]

[a]*Department of Materials Science and Engineering, National Tsing Hua University, Hsinchu, Taiwan*
[b]*Department of Chemistry, National Taiwan University, Taipei, Taiwan*

Abstract

A 10 MHz electrochemical quartz crystal microbalance (EQCM) was employed to study the hydrogen absorption–desorption behavior in Pd and $Pd_{77}Ag_{23}$ films. Each film of thickness varying from 100 to 200 nm was deposited on an AT-cut quartz crystal by magnetron sputtering. It was electrolytically charged–discharged with hydrogen in 0.1 M KOH solution by cyclic voltammetry at room temperature. The hydrogen absorbed or desorbed in the film was measured by EQCM through the variation of the oscillation frequency. The frequency shift is caused by the synergistic effect of mass increase (or decrease) and the stress induced by hydrogen absorption in the film. Based on the integrated oxidation current, the amount of hydrogen in the film was calculated. The magnitude of stress in the film could then be estimated from the frequency shift. The kinetic curves of hydrogen absorption at various reduction potentials were also obtained and compared for Pd and $Pd_{77}Ag_{23}$ films. The $Pd_{77}Ag_{23}$ film had a faster hydrogen absorption rate but absorbed less hydrogen than the Pd film. It was also found that the hydrogen absorption rates in both films were controlled predominantly by the surface effect and hydrogen fugacity.

Keywords: EQCM; Pd; $Pd_{77}Ag_{23}$; Thin film; Stress; Diffusion

1. Introduction

Since Sauerbrey [1] reported the theory and application of the quartz crystal microbalance (QCM) in 1959, it has become a popular method for studying the gas absorption behavior in thin films [2–4]. In 1981, Nomura et al. [5,6] applied the equipment in liquid to measure the mass change at the electrode surface. Many characteristics and applications of the electrochemical quartz crystal microbalance (EQCM) have been examined [7–9].

Recently, Li and Cheng observed, in situ, the hydrogen absorption–desorption processes and reduction–oxidation reactions in La–Ni thin film electrodes [10]. Traditionally, the thin film stress must be obtained by using quartz crystals of two orientations (i.e., AT- and BT-cut quartz crystals) [11]. In the present study, we have developed another method to monitor the hydrogen absorption–desorption behavior in thin films in situ. This method provides direct evidence of the hydrogen occlusion mechanism and separates the mass effect from the thin film stress in the frequency shift. The well-known element Pd [2,12,13] and the higher permeability material $Pd_{77}Ag_{23}$ [14,15] are used to investigate and compare hydrogen occlusion behaviors [16].

2. Experimental details

Polished AT-cut quartz crystals were used as the substrates. Each has a fundamental frequency of 10 MHz and both sides of each crystal are coated with gold. The gold electrode has a thickness of 100 nm and a diameter of 0.5 cm. A Pd or $Pd_{77}Ag_{23}$ film was deposited on one side of the gold by magnetron sputtering to form a double-layer structure (Pd/Au or $Pd_{77}Ag_{23}$/Au). The sputtering chamber was first evacuated to 1.33×10^{-3} Pa and then charged with Ar at a pressure of 0.93 Pa during the sputtering. The thickness of the Pd or $Pd_{77}Ag_{23}$ film was determined by a profilometer. A 5 ml three-compartment glass cell with 0.1 M KOH solution as the electrolyte was used for the EQCM experiment. The counter and reference electrodes were Pt and Ag/AgCl, respectively, and the Pd/Au or $Pd_{77}Ag_{23}$/Au film coated on the quartz crystal was used as the working electrode. The opposite side of the quartz crystal without the Pd or $Pd_{77}Ag_{23}$ coating was exposed to air. Prior to the test, the electrolyte was de-

*Corresponding author.

0925-8388/99/$ – see front matter
PII: S0925-8388(99)00340-0

aerated by continuous bubbling of nitrogen gas for 15 min and the potential was adjusted to stabilize the frequency of the working electrode. The cyclic voltammetry was set to scan from 0 to −1.5 V, and then back to 0 V at a rate of 5 mV/s. Some tests were performed at constant potentials (−1.1, −1.2, −1.3, −1.4, or −1.5 V) to study the kinetics and capacity of hydrogen uptake. The frequency and current signals from the electrode were transferred to a personal computer through an A/D-D/A interface card so that the potential could be controlled by the computer program.

3. Results and discussion

The curves of the electrochemical current and frequency shift for Pd are shown in Fig. 1. Based on the laws of mass conservation and charge conservation, the frequency shift and electrochemical current are dependent on the amount of hydrogen occlusion in the film. From the frequency shift, four processes, adsorption at the surface, absorption in the bulk, desorption from the surface and desorption from the bulk of hydrogen in the film, were monitored in situ, with the electrochemical current being accompanied by the frequency shift. In the charging period, hydrogen adsorbs on the film surface at below 0.78 V. The film then absorbs hydrogen when the potential goes into the reduction region and the curve of the electrochemical current rises rapidly. The frequency shift also increases until equilibrium is reached, which means that the concentration of hydrogen in the film has been saturated. In other words, hydrogenation has approached a stable state and the phase transformation is finished. Subsequently, when the potential scans back to 0 V, hydrogen desorbs from the surface layer of the film. The electrochemical oxidation current returns to zero. After the current has passed through the zero current point, a broad peak of oxidation current is observed. The frequency shift also gradually decreases to zero. The maximum integrated oxidation current and its corresponding potential can be treated as performance indices of a metal-hydride battery [17].

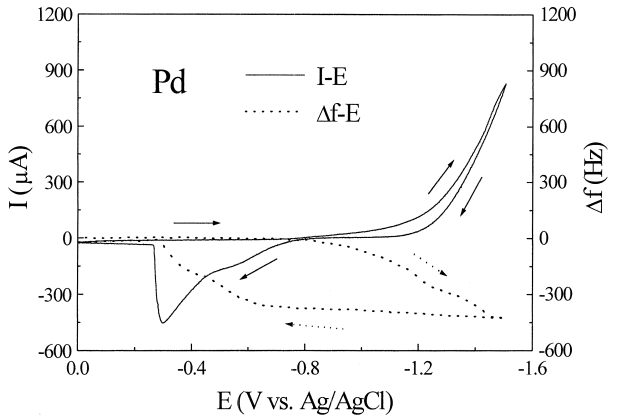

Fig. 1. Electrochemical current and the resonant frequency shift during the potential scan for a Pd film. Thickness: 120 nm.

In effect, the frequency shift is a result of several factors [18]: mass effect (Δf_m), stress effect (Δf_s), viscosity effect (Δf_v), and roughness effect (Δf_r). Adjusting the potential of the working quartz crystal can eliminate the viscosity and roughness effects, and the total frequency shift can be described by

$$\Delta f = \Delta f_m + \Delta f_s \quad (1)$$

According to Sauerbrey's equation [1], the mass effect can be written as

$$\Delta f_m = -\Delta m \times f_q/(\rho_q \times t_q) \quad (2)$$

where Δm is the mass of a unit area and the area is 0.1963 cm^2, f_q is the fundamental frequency of the quartz crystal (10 MHz), ρ_q is the density of the quartz crystal (2.649 g/cm^3), and t_q is the thickness of the quartz crystal (0.0166 cm). EerNisse [11] reported that the thin film stress could be written as

$$\Delta f_s = k\Delta S \times f_q/t_q \quad (3)$$

where k is the stress coefficient (2.75×10^{-12} cm^2/dyn for AT-cut orientation) and ΔS is the surface tension (dyn/cm). The average thin film stress τ_f is derived by dividing the surface tension ΔS by the thickness t_f of the thin film:

$$\tau_f = \Delta S/t_f \quad (4)$$

where the average thickness of the Pd thin film studied here is 120 nm. If the mass of hydrogen occluded in the film is known, the frequency shift due to the mass effect Δf_m is calculated using Eq. (2). Thus, the surface tension can be obtained from Eqs. (1) and (3). It is easy to determine the thin film stress by substituting surface tension in Eq. (4).

From Fig. 1, both the frequency shift and electrochemical current change little from 0 to −0.8 V because the amount of hydrogen adsorption is very small. Beyond the potential −0.78 V, the hydrogen absorption induces a linear decrease of frequency to −423 Hz. At the same time, the reduction current is also raised rapidly at a constant rate even after the frequency shift has reached a stable state. To reach a shift of −423 Hz, a reduction current of 650 μA is observed. When the potential was scanned back to 0 V, the process of hydrogen desorption from the surface was observed. The maximum oxidation current was −454 μA at a potential of −0.3 V. Incidentally, the dehydrogenation scan can be treated as a measure to calculate the output power of thin film batteries. The maximum oxidation potential can be treated as output voltage to limit the output of the current. It provides a convenient way of evaluating the performance of metal-hydride batteries.

When the oxidation current during the reverse scan is integrated, the mass of hydrogen desorbed from the film is calculated to be 181 ng. Based on the weight of the Pd

film, this is equivalent to a concentration of H/Pd=0.67. From Eq. (2), the frequency shift due to the mass effect is 210 Hz. With the total frequency shift being 423 Hz, the difference of 213 Hz can be ascribed to the stress effect. According to Eqs. (3) and (4), the stress is calculated to be 1071 MPa. This value is about the same as that reported by Cheek and O'Grady [12]. The tensile strength of Pd is only 200 MPa [19]. Therefore, the chemical reaction of hydrogen with the Pd film induces a stress larger than the tensile strength by a factor of 4. Based on this method, it is seen that the mass and stress effects can be separated from a single specimen.

Silver has often been used as an alloying element in Pd to increase the permeability of hydrogen or to suppress the critical temperature of the miscibility gap of Pd–H. Among the Pd–Ag alloys, the composition $Pd_{77}Ag_{23}$ is especially attractive [20]. The relation between the electrochemical current and the frequency shift during potential sweeping for a $Pd_{77}Ag_{23}$ film of average thickness 175 nm is shown in Fig. 2. By comparing with that of Pd, the frequency shift in the range of hydrogen adsorption (0 to −1.0 V) is larger by about 18.5%. The rate of the frequency shift in $Pd_{77}Ag_{23}$ is faster than that in Pd at the hydrogen absorption stage (−1.0 to −1.23 V), and the total frequency shift due to hydrogen absorption (435 Hz) is larger than that of the Pd film. The start potential for hydrogen absorption is −1.0 V, more negative than that of Pd (−0.8 V). Therefore, the addition of Ag results in an increase of the hydrogen absorption rate. For the process of desorption from the surface (−1.23 to −0.6 V), the rate of the frequency shift is also faster than that of Pd by 19.5%. The total oxidation current calculated from the $P_{77}Ag_{23}$ film is 126 ng, so that the atomic ratio (H/M) for hydrogen absorption to $Pd_{77}Ag_{23}$ is 0.34. The corresponding frequency shift of the mass effect is 146 Hz, and the frequency shift due to the stress effect is 289 Hz. The thin film stress induced by hydrogen in $Pd_{77}Ag_{23}$ is calculated to be 997 MPa, a little lower than in Pd.

To study further the behavior of hydrogen diffusion in the films, the kinetic curves of the frequency shift of Pd and $Pd_{77}Ag_{23}$ at various potentials are shown in Figs. 3 and 4, respectively. All potentials for these kinetic curves were selected from the hydrogen reduction region. From these kinetic curves, it is seen that, as the potential becomes more negative, the absorption rate becomes more rapid. The frequency shifts are not sensitive to the potentials. The electrochemical driving force appears to enhance the hydrogen absorption rate, but not the concentration of hydrogen. According to Figs. 1 and 2, the electrical resistances calculated from the reduction region are constant for Pd and $Pd_{77}Ag_{23}$ (309 and 411 Ω, respectively). Therefore, the potential in the reduction region is proportional to the current. At any one potential from −1.2 to −1.5 V, for example at −1.3 V, the hydrogen absorption rate in $Pd_{77}Ag_{23}$ is twice that in Pd. It takes 20 s to reach equilibrium in Pd but only 10 s in $Pd_{77}Ag_{23}$ to reach the steady state. The addition of Ag to Pd changes the surface characteristics and increases the rate of hydrogen absorption. Based on the diffusion coefficient of hydrogen in bulk Pd [21], the diffusion rate deduced from this study is much lower by about two

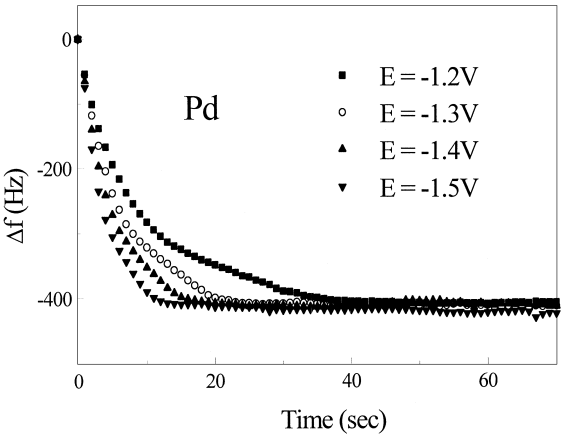

Fig. 3. Hydrogen absorption kinetic curves at constant potential for a Pd film.

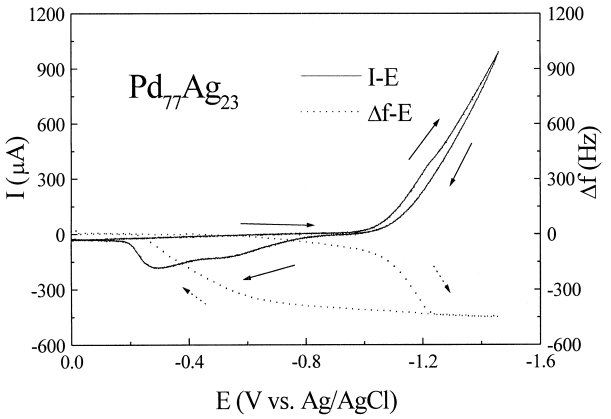

Fig. 2. Electrochemical current and the resonant frequency shift during the potential scan for a $Pd_{77}Ag_{23}$ film. Thickness: 175 nm.

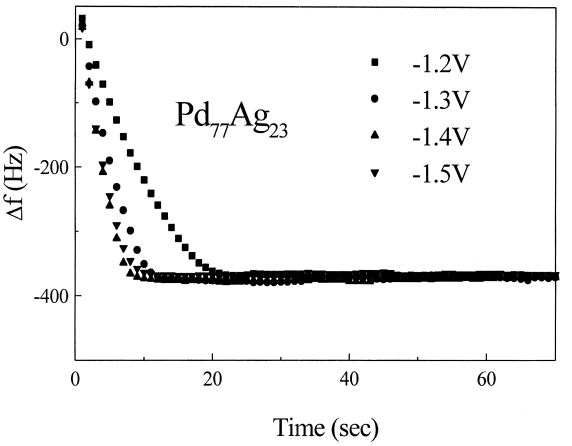

Fig. 4. Hydrogen absorption kinetic curves at constant potential for a $Pd_{77}Ag_{23}$ film.

orders of magnitude. The fugacities of hydrogen at these potentials in the electrochemical method are >5000 atm in the gaseous state [22]. It is believed that the surface effect is the dominating factor controlling hydrogen absorption in the films in this study.

4. Conclusions

The processes of adsorption, absorption, desorption from the surface and from the bulk of hydrogen occlusion in a Pd or $Pd_{77}Ag_{23}$ film has been observed in situ by EQCM. The thin film stress can be obtained from a single AT-cut quartz crystal by subtracting the mass effect from the total frequency shift. The $Pd_{77}Ag_{23}$ film has a faster hydrogen absorption rate but occludes less hydrogen than the Pd film. The surface effect is expected to be the rate controlling process for hydrogen occlusion into the films.

Acknowledgements

This work was supported by the National Science Council of ROC under contract Nos. NSC 87-2216-E-007-019 and NSC 87-TPC-M-002-001 and the National Tsing Hua University Fellowship 82-2-1.

References

[1] G. Sauerbrey, Z. Phys. 155 (1959) 206.
[2] R.V. Bucur, T.B. Flanagan, Z. Phys. Chem. 88 (1974) 225.
[3] H. Sakaguchi, N. Taniguchi, H. Nagai, K. Niki, G. Adachi, J. Shiokawa, J. Phys. Chem. 89 (1985) 5550.
[4] H. Sakaguchi, N. Taniguchi, H. Seri, J. Shioawa, G. Adachi, J. Appl. Phys. 64 (1988) 15.
[5] T. Nomura, Anal. Chim. Acta 124 (1981) 81.
[6] T. Nomura, T. Nagamune, K. Izutsu, T.S. West, Bunseki Kagaku 30 (1981) 494.
[7] S. Bruckenstein, M. Shay, Electrochim. Acta 30 (1985) 1295.
[8] W. Wicke, J. Blaurock, J. Less-Common Met. 130 (1987) 351.
[9] J. Mcbreen, J. Electroanal. Chem. 287 (1990) 279.
[10] Y. Li, Y.-T. Cheng, J. Electrochem. Soc. 143 (1996) 120.
[11] E.P. EerNisse, J. Appl. Phys. 43 (1971) 1330.
[12] G.T. Cheek, W.E. O'Grady, J. Electroanal. Chem. 277 (1990) 341.
[13] L. Schlapbach, Hydrogen in Intermetallic Compounds, Vol. II, Springer, Berlin, 1992.
[14] A. Sieverts, E. Jurish, A. Metz, Z. Allg. Chem. 92 (1915) 4.
[15] A. Sieverts, E. Jurish, H. Hagen, Z. Phys. Chem. 174A (1935) 247.
[16] Y. Fukai, The Metal–Hydrogen System, Springer, New York, 1993.
[17] T. Sakai, H. Ishikawa, H. Miyamura, N. Kuriyama, J. Electrochem. Soc. 138 (1991) 908.
[18] V. Tsionsky, L. Daikhin, E. Gileadi, J. Electrochem. Soc. 143 (1996) 7.
[19] H.E. Boyer, T.L. Gall (Eds.), Metals Handbook Desk Edition, ASM International, 1984, p. 13.2.
[20] G.J. Grasshoff, C.E. Pilkington, C.W. Corti, Platinum Met. Rev. 27 (1983) 157.
[21] J. Voelkl, G. Wollenweber, K.-H. Klatt, G. Alefeld, Z. Naturforsch. a 26 (1971) 922.
[22] B. Baranowski, Ber. Bunsenges. Phys. Chem. 76 (1972) 714.